Canadian Science Publishing | Canadian Journal of Fisheries and Aquatic Sciences

Size selectivity and length-dependent escape behaviour of haddock in a sorting device combining a grid and a square mesh panel

Journal:	*Canadian Journal of Fisheries and Aquatic Sciences*
Manuscript ID	cjfas-2017-0461.R2
Manuscript Type:	Article
Date Submitted by the Author:	30-Aug-2018
Complete List of Authors:	Herrmann, Bent; SINTEF Fisheries and Aquaculture, Fishing Gear Technology Sistiaga, Manu; SINTEF Fisheries and Aquaculture, Fisheries Technology Grimaldo, Eduardo; SINTEF Ocean, Fisheries Technology; SINTEF , Larsen, Roger; The Arctic University of Norway UIT, The Norwegian College of Fishery Science; Olsen, Leonore; SINTEF Nord Brinkhof, Jesse ; The Arctic University of Norway, The norwegian College of Fisheries Sciences Tatone, Ivan; University of Tromsø, Norwegian College of Fisheries and Aquatic Sciences
Keyword:	sorting grid, square mesh panel, combined size selection, haddock, contact probability
Is the invited manuscript for consideration in a Special Issue? :	Not applicable (regular submission)

Size selectivity and length-dependent escape behaviour of haddock in a sorting device combining a grid and a square mesh panel

Bent Herrmann[1,2*&], Manu Sistiaga[1&], Eduardo Grimaldo[1&], Roger B. Larsen[2&], Leonore Olsen[3], Jesse Brinkhof[2], Ivan Tatone[2]

[1] SINTEF Ocean, Brattørkaia 17C, N-7010 Trondheim, Norway

[2] The Arctic University of Norway, UiT, Breivika, N-9037 Tromsø, Norway

[3] SINTEF Nord, Storgata 118, 9008 Tromsø, Norway

*E-mail address: bent.herrmann@sintef.no

[&] Equal authorship

Abstract

Size selectivity of a new sorting section combining a sorting grid and a square mesh panel was tested for haddock (*Melanogrammus aeglefinus*) in the Barents Sea demersal trawl fishery. Sampling data for a wide size range enabled investigating the selection process for this species in detail, both for the grid and the square mesh panel. Contrary to earlier studies modelling size selectivity for grids and square mesh panels, which assume that the escape behaviour of all sizes of fish is equal, we applied a model that accounted for that haddock of different sizes can show different escape behaviour. Our results demonstrated that this model could describe the experimental data collected better than existing models. Specifically, our results showed that the likelihood for smaller haddock to seek escape through the grid and the square mesh panel was higher than for bigger haddock that still would manage to escape through the devices if they

attempted. The new modelling approach presented in this study may be applicable to other species, selection devices and fisheries.

Keywords: sorting grid; square mesh panel; combined size selection; haddock; contact probability

Introduction

In many demersal trawl fisheries, size and/or species selection in the codend is suboptimal for the intended exploitation pattern, which leads to discards in fisheries (Kelleher, 2005). One strategy to reduce the catch of unwanted sizes and/or species in demersal trawl fisheries is to improve the selectivity in the fishing gear used. While codend selection is the most widespread form for selectivity in trawls (Glass, 2000), in several trawl fisheries it has been supplemented by one or more selection devices installed in the section in front of the codend or in the codend itself.

Square mesh panels (Broadhurst, 2000; Catchpole and Revill, 2008; Alzorriz et al., 2016; Graham and Kynoch, 2001; Krag et al., 2016, 2017; Brčić et al., 2016; Santos et al., 2016; Zuur et al., 2001; O'Neill et al. ,2006) and sorting grids (Sistiaga et al., 2010; Herrmann et al., 2013; Lövgren et al., 2016; Jørgensen et al., 2006; Larsen and Isaksen, 1993) are technical devices often used to supplement codend size and/or species selection in demersal trawls. In some trawl fisheries, the use of such additional selection devices has become mandatory. For example, in the Barents Sea bottom trawl fishery targeting cod (*Gadus morhua*) and haddock (*Melanogrammus aeglefinus*), the compulsory size selectivity system consists of a section with a 55 mm bar spacing sorting grid followed by a codend with a minimum mesh size of 130 mm (Larsen et al., 2018). In this fishery, several studies have evaluated the efficiency of different grid configurations on cod and haddock (Larsen et al., 2018; Sistiaga et al., 2010).

Both fish behaviour and fish morphology affect the sorting efficiency and size selectivity of a specific selection device (Sistiaga et al., 2011), and both aspects have been widely investigated in relation to the selectivity of cod and haddock in trawls. Specially, haddock is one of the most studied species regarding escape behaviour in demersal trawls (Wardle, 1993; Krag et al., 2010; Winger et al., 2010). Several studies on this species include the effect and efficiency of inserting square mesh panels in the trawl. Many of these studies were conducted by Marine Scotland (formerly Fisheries Research Service) and an overview can be found in Fryer et al. (2016). Haddock is widely distributed in the North Atlantic with important commercial fisheries in both European and North American waters (Fryer et al., 2016). Therefore, it is of broad interest and relevance to improve the knowledge and methods applied to quantify escape behaviour and size selectivity of this species.

Former studies modelling size selectivity of square mesh panels and grids for haddock and other species have quantified the behavioural aspect of the process by a factor termed "contact". Contact is quantified as the fraction of species that contact the selection device while passing through the trawl that leads to a size-dependent probability of escape. Earlier studies have all assumed/approximated the contact factor to a fixed value and have not allowed it to vary with fish size (Zuur et. al, 2001; O'Neill et al., 2006; Sistiaga et al., 2011, 2017; Larsen et al., 2018). However, several studies in the literature have documented that haddock of different sizes may exhibit different behaviour in a trawl (Grimaldo et al., 2018; Melli et al. 2017, 2018). Therefore, it is relevant to investigate if a modelling approach that avoids the assumption of length independency on the behavioural aspect can improve the modelling of size selectivity processes for haddock in relation to grids and square mesh panels in trawls. Further, such a modelling approach would contribute with new quantitative knowledge about the escape behaviour of haddock in relation to sorting grids and square mesh panels.

One of the aims of the present investigation is to discern why former studies have not found the need to account for size-dependent escape behaviour of haddock. Specifically, do all sizes of haddock have a similar escape behaviour in reaction to a grid or a square mesh panel, or was the size range of haddock that could potentially utilize the selection device to escape too narrow, therefore representing the contact factor by a fixed value being a good approximation?

Based on the considerations described above, the main purpose of the current study was to investigate, model and quantify escape behaviour and size selectivity of haddock in a new sorting section containing both a grid and a square mesh panel. The study was based on collecting size selectivity data for the new sorting section in the Barents Sea demersal trawl fishery, and quantifying how this new system performed including comparisons with the compulsory grid-based sorting systems in this fishery. Specifically, our main objectives were to:

- Determine if there is size-dependent escape behaviour for haddock though the grid and square mesh panel, and if it is the same for both devices.
- Determine how any behavioural differences affect size selectivity for the grid and square mesh panel, respectively.
- Describe to what extent the grid and square mesh panel each contributes to the combined size selection in the new sorting section.

Materials and methods

Sorting system

The new sorting design tested in this study combined a sorting grid and a square mesh panel. It was based on the Sort-V single grid system already used in the Northeast Atlantic gadoid fishery (Jørgensen et al., 2006). A detailed description of the Sort-V sorting system is provided in Herrmann et al. 2013 and in Grimaldo et al. 2018. In the new sorting section, the grid was installed upside down compared to the original Sort-V section. In addition, the top panel in the grid section was substituted by a square mesh panel. We hypothesized that placing the steel grid in the lower panel would allow it to sort fish while also acting as a lifting panel to guide fish towards the square mesh panel. The new sorting system was built on a four-panel section made of 138 mm nominal mesh size (nms) knotted diamond mesh netting (Euroline Premium Polyethylene (PE), single Ø 8 mm braided twine). It was 29.5 meshes long (approx. 4.6 m) and had 80 meshes of circumference (approx. Ø 1.2 m). All four selvedges were strengthened by 30 mm Danline PE ropes. A standard 55 mm bar spacing sorting grid of Sort-V type (1650 mm × 1234 mm) was installed in the section with an inclination angle of 23° ± 2° (Fig. 1). According to earlier studies (Kvamme and Isaksen 2004; Isaksen, 1998; Sistiaga et al., 2010) the optimal grid angle is between 23 and 26 degrees. The original top panel in the section was replaced by a square mesh panel made of single Ø 8 mm braided knotless Ultracross netting. The panel was 50 meshes long (~3.5 m) and 17 meshes wide (~1.2 m) (Fig. 1).

Fig. 1.

The average mesh size of the square mesh panel was estimated from 40 measurements (2 × 20 mesh rows) taken with an ICES gauge applying a force of approximately 4 kg (Westhoff et al., 1962). Mean mesh size was 144.30 ± 2.43 mm (mean ± SD).

Research vessel, study area, and gear set-up

Experimental fishing was conducted on board the research vessel "Helmer Hanssen" (63.8 m LOA and 4080 HP) between the 6th and 15th of March 2017. The fishing grounds chosen for the tests were off the coast of Finnmark (Northern Norway) between 70˚29'–70˚52'N and 30˚08'–31˚44'E. The towing speed during the trials was 3.5 – 4 knots. The fishing operation was carried out around the clock at depths that ranged between 320-365 m implying complete darkness for all hauls.

We used an Alfredo No. 3 two-panel Euronete trawl built entirely of 155 mm nms PE netting (single Ø 4 mm braided knotted twine). The trawl had a headline of 36.5 m, a fishing line of 19.2 m, and 454 meshes of circumference at the trawl mouth. It was rigged with a set of bottom trawl doors (Injector Scorpion type, 8 m^2, 3200 kg each), 60 m sweeps, 28.5 m long bridles (Ø 16 mm), and a 111 m long ground gear. The sides of the ground gear had five 53 cm diameter steel bobbins distributed on a 46 m chain (Ø 19 mm), and the centre of the ground gear had a 19.2 m long rockhopper (with 53 cm rubber discs) that was attached to the fishing line of the trawl.

We built a diamond mesh transition section to connect the two-panel trawl belly to the four-panel sorting section. It was made using 138 mm nms Euroline Premium PE knotted netting (single Ø 8.0 mm braided twine) and was 35.5 meshes long. A four-panel diamond-mesh codend was attached after the sorting section. It was made from 138 mm nms Euroline Premium PE knotted netting (Polar Gold) (single Ø 8 mm braided twine). The codend was 40 meshes long (approx.

6.2 m) and had 64 open meshes in circumference (approx. Ø 1 m). All four selvedges were strengthened by 30 mm Danline PE ropes. The codend had round straps placed every 1.20 m along all its length. The round straps were 6.9 m long, which limited the expansion of the codend to 2.20 m diameter. Because we wanted to evaluate the selectivity properties of the sorting section alone, the codend was blinded by an inner-net constructed of 48 mm Euroline Premium PE knotted netting (Ø 2.2 mm single twine). The inner-net was 300 meshes around, and the difference in meshes around the codend and the inner-net, in addition to the round straps, limited expansion of the codend during the fishing operations. This limitation guaranteed a low opening angle of the diamond meshes in the inner-net, which was estimated to be <28 degrees. Using this maximum opening angle for a diamond mesh of 48 mm and morphological data obtained with the FISHSELECT simulation tool (Herrmann et. al 2009) in Sistiaga et al. (2011), we estimated that no haddock above 13.5 cm in length would be physically able to escape through the inner-net netting.

We applied the covered-gear method (Wileman et al., 1996; Grimaldo et al., 2016) and used two covers to collect all fish escaping through the grid (grid cover) and the square mesh panel (panel cover) (Fig. 2). The front part of the covers was made of square meshes of Dyneema netting (knotless 210/54 braided twine). The purpose of the netting material was twofold: i) to ensure that the water flow outside the trawl did not push the cover against the square mesh panel or the grid outlet and ii) to create enough water flow through the meshes to push the fish entering the covers to the cover codend. The back part of the covers was made of diamond meshes of Polyamid PA netting (2.5 mm Ø knotted braided twine). The average mesh size of the covers was estimated from 80 measurements (2 × 20 mesh rows in each of the covers) taken with an ICES gauge (Westhoff et al. 1962). Mean mesh size was 57.41 ± 0.97 mm (mean ± SD). In the last 2 m of the cover, where we expected fish to come in contact with the cover netting, we installed a small mesh size inner-net made of approximately 10 mm meshes to ensure that the smallest fish would not be able to escape from the cover net. The total length of the covers was approximately 18 m. At the front of the panel cover we attached six plastic floats (Ø 20 cm and approx. 2.8kg buoyancy each) to ensure that it expanded and stayed clear of the panel. At the grid cover, 16 kg of chains were fixed to the lower panel to secure its opening. Due to that the expanding forces needed in the covers were vertical (both upwards and downwards), we used floats and chains to keep the covers clear from the gear except for kites (see Fig. 2). Floats and chains are easier to install, cheaper and give the possibility to make adjustments easier than with kites. Therefore, they were the preferred option. The floats and chains used were equivalent to the spreading force of the kites used in the tank.

Fig. 2.

All haddock > 10 cm in total length present in the codend or the covers were measured to the nearest centimetre.

Modelling the size selectivity for the sorting devices

For a fish to escape through a selection device two conditions need to be fulfilled: i) the fish needs to make contact/seek escape through the device; ii) it needs to be morphologically able to pass through the device (Herrmann et al., 2009). When modelling size selectivity/retention probability $r_{device}(l)$ for a selection device like a square mesh panel or a sorting grid, the first condition has traditionally been accounted by a fish size-independent constant contact factor

(C_{device}) (Sistiaga et al., 2010). C_{device} holds a constant value that ranges between 0.0 (no fish make contact) and 1.0 (all fish make contact). The second condition often has been modelled by a logistic curve defined by the parameters $L50_{device}$ (length of fish with 50% retention probability conditioned making contact) and SR_{device} (= $L75_{device} - L25_{device}$) (Wileman et al., 1996):

$$r_{device}(l, C_{device}, L50_{device}, SR_{device}) = 1.0 - \frac{C_{device}}{1.0 + exp\left(\frac{ln(9)}{SR_{device}} \times (l - L50_{device})\right)} \qquad (1)$$

In model (1) l represents the length of the fish. Examples for using (1) to model size selectivity in a trawl section with a square mesh panel include Zuur et al. (2001), O'Neill et. al (2006), Alzorriz et al. (2016), Brčić et al. (2017), Santos et al. (2016) and Krag et al. (2016, 2017), whereas examples for modelling size selectivity in sorting grids include Sistiaga et al. (2010, 2016), Herrmann et al. (2013), Grimaldo et al. (2015), Brčić et al. (2015), Stepputtis et al. (2016), Lövgren et al. (2016) and Larsen et al. (2016, 2017, 2018). A shared limitation for all these selectivity studies is that all sizes within the species investigated were assumed to be equally likely to seek escape/contact with the selection device investigated. For fish so big that they would not be able to morphologically pass through the selection device, the specific value for the C_{device} will not matter as their morphology will anyway prevent escape. Contrary, for fish that can morphologically pass through the selection device, potential size dependency in escape behaviour will affect the contact probability with the selection device and consequently the selection process. Thus, to be able to account for potential differences in escape behaviour for haddock of different sizes, in addition to using model (1) with a constant for C_{device} we also considered the length-dependent model previously proposed by Krag et al. (2014). Krag et al. (2014) used this length-dependent model to model the length-dependent probability for fish to contact a large mesh panel installed in a trawl selection. The latter model contains four parameters ($C1_{device}$, $C2_{device}$, $L50C_{device}$, and SRC_{device}):

$$C_{device}(l) = C1_{device} + (C2_{device} - C1_{device}) \times \frac{exp\left(\frac{ln(9)}{SRC_{device}} \times (l - L50C_{device})\right)}{1.0 + exp\left(\frac{ln(9)}{SRC_{device}} \times (l - L50C_{device})\right)} \qquad (2)$$

Equation (2) is a flexible formula that enables modelling increasing, decreasing and constant values for C_{device} *(l)*. $C1_{device}$ and $C2_{device}$ are constants constrained to the interval [0.0;1.0] that represent the asymptotic contact values for respectively fish of smallest and largest sizes. $L50C_{device}$ is the fish length at which C_{device} *(l)* is the mean of $C1_{device}$ and $C2_{device}$. SRC_{device} defines how quickly C_{device} *(l)* shifts from a value close to $C1_{device}$ to a value close to $C2_{device}$ with increasing fish length in the vicinity of $L50C_{device}$. Thus, if SRC_{device} is close to *0.0*, the change in C_{device} *(l)* will appear over a small length range, whereas if SRC_{device} holds a value far from 0.0 the change in C_{device} *(l)* will cover a wider length span. Fig. 3 shows examples on some of the different length-dependent escape attempt patterns that can be modelled based on (2), and how (2) can lead to different size selection curves when it is applied for C_{device} in model (1).

FIG. 3

In this study, we use model (1) with model (2) to model separately the size selection for both the sorting grid and the square mesh panels for standalone deployments. Further, in the preceding section we outlined how this leads to modelling the selection patterns in the complete sorting section consisting of both the sorting grid and the square mesh panel. This includes how the corresponding sets of model parameters ($L50_{grid}$, SR_{grid}, $C1_{grid}$, $C2_{grid}$, $L50C_{grid}$, SRC_{grid}) and ($L50_{panel}$, SR_{panel}, $C1_{panel}$, $C2_{panel}$, $L50C_{panel}$, SRC_{panel}) are estimated for respectively the sorting grid (*device* = *grid*) and the square mesh panel (*device* = *panel*).

Describing the selection patterns for the sorting section and parameter estimation

The selection process in the sorting section can be considered dual sequential with an initial escape option through the grid followed by an escape option through the square mesh panel for those fish that did not escape through the grid. The fish that do not escape through the grid nor the square mesh panel, end up being retained in the blinded codend. The experimental data are length class-wise (l) collected in three fractions: i) number escaped through the grid (ng_l); ii) number escaped through the square mesh panel (np_l); and iii) number retained in the blinded codend (nc_l). Therefore, to model the experimentally collected size selection data we needed to quantify the length-dependent probabilities $e_{grid}(l)$, $e_{panel}(l)$ and $r_{codend}(l)$, which express the probability for a fish that enters the sorting section to be collected in respectively the cover over the grid, the cover over the square mesh panel and in the codend. Using model (1) for $r_{device}(l)$ and model (2) for $C_{device}(l)$ for both the grid and square mesh panel selection processes, we arrive at:

$$\begin{gathered} e_{grid}(l) = 1.0 - r_{grid}\left(l, C_{grid}(l), L50_{grid}, SR_{grid}\right) \\ e_{panel}(l) = r_{grid}\left(l, C_{grid}(l), L50_{grid}, SR_{grid}\right) \times \left(1.0 - r_{panel}\left(l, C_{panel}(l), L50_{panel}, SR_{panel}\right)\right) \\ r_{codend}(l) = 1.0 - e_{grid}(l) - e_{panel}(l) \end{gathered} \quad (3)$$

The special case with constant $C_{grid}(l)=C1_{grid}$ and $C_{panel}(l)=C1_{panel}$ was considered first for modelling the size selectivity in the new sorting section before using the more flexible model (2). The values for the parameters for the overall model (3) were obtained using Maximum Likelihood (ML) estimation based on the experimental data pooled over hauls j (1 to m) by minimizing:

$$-\sum_l \sum_{j=1}^{m} \left\{ ng_{l,j} \times ln\left(e_{grid}(l)\right) + np_{l,j} \times ln\left(e_{panel}(l)\right) + nc_{l,j} \times ln\left(r_{codend}(l)\right) \right\} \quad (4)$$

where $ng_{l,j}$, $np_{l,j}$, and $nc_{l,j}$ denote the number of haddock caught in haul j with length l that were collected in the cover for the grid, the cover for the square mesh panel, and the blinded codend, respectively (Fig. 2). Determination of goodness of fit of the model selected to describe the experimental data was based on the p-value, model deviance versus degrees of freedom (DOF), and visual inspection of the ability of the model curves to reflect the length-based trends in the data (Larsen et al., 2016). A p-value < 0.05 and deviance >> DOF would indicate poor model fit making it unlikely that the observed deviations between the modelled selectivity curves and the experimental rate are coincidental. Another symptom of poor description of the experimental data is visual disability of the modelled curves to represent the fish size-dependent experimental rates. Akaike information criterion (AIC) values (Akaike, 1974) for the model fits were calculated to help compare the feasibility of using a model with length-independent and length-dependent contact for the grid and square mesh panel size selection. The model with lowest AIC was preferred.

The ML estimation using expression (4) with (3) requires aggregation of the experimental data over hauls. This results in stronger data to estimate the average size selectivity, but it does not explicitly consider between-haul variation in selectivity (Fryer, 1991). To account correctly for the effect of between-haul variation in the estimation of the uncertainty in size selection, we estimated Efron percentile confidence intervals (CIs) (Efron, 1982; Chernick, 2007) for both the estimated parameters in equation (3) and the resulting curves for $e_{grid}(l)$, $e_{panel}(l)$, and $r_{codend}(l)$ (as well $r_{grid}(l)$ and $r_{panel}(l)$) for the standalone deployment size selection curves) using a double bootstrap method. We used the software tool SELNET (Herrmann et al., 2013) for the analysis and applied 1000 bootstrap iterations for the estimation of the CIs.

Investigation of whether a reduced length span in experimental data can hide length-dependency in contact probability

Because our data ultimately needed a model with size-dependent contact probability and previous studies have used a model with constant contact probability without reporting problems, we wanted to investigate whether this need could be related to the size range of haddock in the experimental sampling. Therefore, we investigated the ability of model (1) with a size-independent contact to describe the experimental data for the combined size selection in the sorting section, for the grid alone, and for the square mesh panel alone while ignoring the smallest length classes in the collected haddock data. We did this in steps of 5 cm until no haddock < 30 cm were considered in the estimation. For each step, we estimated the p-value, which quantifies the probability of obtaining at least as a big discrepancy between the modelled selectivity curves and experimental data by coincidence. Further, for each case we visually inspected how well the modelled curves reflected the length-dependent patterns in the experimental data.

Results

During the sea trials we carried out 20 valid hauls, and we caught and length measured a total of 11,189 haddock between 10 and 70 cm (Table 1). Only 23 haddock (0.2%) were below the 13.5 cm length class (where we could not rule out release through the codend inner-net with a 100% certainty), making the effect of these on the estimated size selectivity negligible. The two other main species caught were cod (2958 individuals) and redfish (1331 individuals). The data for these species are not presented in this study as the numbers of individuals caught for certain ranges in their length spans were not high enough for the analysis carried out in this study. However, results for these species are provided in Sistiaga et al. (2017).

Table 1.

Size selection of haddock was estimated by fitting the model described by equation (1) to the haul data summarised in Table 1. This was done first by assuming fish size-independent contact probability for both the grid and the square mesh panel. Table 2 lists the fit statistics, and Figure 4 shows the fit of the model to the experimental data. The fit statistics and visualization of the model fit show clearly that assuming a fish size-independent contact probability was not adequate because the model could not describe the experimental data sufficiently well. Therefore, equation (1), with the fish size-dependent model (2) for contact with the selection devices, was fitted to the experimental data (Table 2; Fig. 4).

Table 2.

Fig. 4.

The fit statistics in Table 2 demonstrate that for the combined dual selection process in the sorting section and the size selection in the grid and for the square mesh panel standalone, the length-dependent contact model was much better at describing the ongoing selection processes than the model that assumes size-independent contact with the devices. In fact, the p-values for the model with constant contacts were < 0.05 for all three cases, meaning that it is unlikely that the observed discrepancies between the modelled curves and the data were coincidental. This premise is further supported by clear patterns in the deviations between the modelled curves and the experimental rates, especially for the grid escape probability (Fig. 4a) and for the retention probability in the codend (Fig. 4c). This contrasts with the results obtained when model (1) was combined with model (2), in which the grid and panel contact probability varied with haddock size. The p-values for the combined size selection, for the grid, and for the square mesh panel in this case are all > 0.05 (Table 2), which implies that the observed discrepancies between modelled curves and experimental rates could be coincidental. The plots in Figure 4 show that the modelled curves reflect the trends in the experimental data well for codend retention (Fig. 4f), grid escapement (Fig. 4d), and square mesh panel escapement (Fig. 4e). The superiority of the length-dependent model for modelling the size selection of haddock in this sorting system was supported by the AIC results. For all three comparisons, the AIC values were much smaller for the length-dependent contact model than for the length-independent contact model (Table 2).

Based on these results, we chose to model the size selection of haddock in the new sorting section based on model (1) with the length-dependent contact model (2). Table 3 shows the parameter values obtained using this model, and Figure 5 shows the size selectivity for the grid (Fig. 5a) and square mesh panel (Fig. 5b) alone. In addition, Figures 5c and 5d show the haddock size-dependent estimated contact probability with the selective devices in the sorting section conditioned that haddock reach the selectivity zone of the device.

Table 3.

Fig. 5.

Figure 5c shows that contact probability with the grid decreased with haddock size between 10 and 35 cm, with the value being very high for the smallest haddock. This is reflected in the low retention rate (Fig. 5a) for sizes of haddock that should be able to escape through the grid ($L50_{grid}$ at 47 cm and SR_{grid} at 7.5 cm) (Table 3). For haddock > 35 cm, only about 33% were estimated to make selectivity contact with the grid, which is reflected in a relatively high retention rate for sizes of haddock that would have at least a 50% chance of escaping (haddock < 47 cm) if they made contact with the grid. These results demonstrate that smaller haddock were more likely to make selectivity contact with the grid than bigger haddock. For the square mesh panel, the smallest haddock also had higher probability for selectivity contact than bigger haddock (Fig. 5d). However, this was only the case for haddock < 20 cm. For haddock > 20 cm the selectivity contact with the square mesh panel was estimated to be approximately 50% for all sizes.

Reduced length span in experimental data can hide length-dependency in contact probability

Model (1) with assumed length-independent selectivity contact with the grid and the square mesh panel was fitted to the experimental data with all haddock below a specific length (i.e., 10, 15, 20, 25 and 30 cm) excluded from the analysis (Fig. 6, Table 4).

Table 4.

Fig. 6.

The p-values in Table 4 clearly show that when haddock < 20 cm were not included in the analysis, the length-independent selectivity contact model produced an acceptable value. In this scenario, the patterns in the deviations between modelled curves and data points disappeared (Fig. 6). This observation explains why previous studies (Sistiaga et al., 2010, 2016) of sorting grids based on haddock that did not sample fish < 20 or 30 cm reported acceptable results for the length-independent selectivity contact model. If these results are not extrapolated to haddock below their sampling limit (20 or 30 cm), they are still valid and not in conflict with the results obtained in this study.

Comparison of the new sorting section with existing grid-based sections

Figure 7 plots the size selection estimated for the new sorting section against results from the literature for the Flexigrid (Sistiaga et al., 2016) (Fig. 7a) and Sort-V (Fig. 7b) systems. This was done to compare the selectivity performance of the new section with the sorting sections applied in the fishery today. For the Flexigrid and Sort-V systems, the comparison was made with results from Sistiaga et al. (2016) and Sistiaga et al. (2010), respectively.

The new sorting section had higher retention rate for a wide span of sizes of haddock, both below and above 40 cm, compared to the Sort-V system (Fig. 7b). The new sorting section and the Flexigrid exhibited very similar size selection for haddock between 20 and 30 cm (Fig. 7a), but for the targeted sizes of haddock (> 40 cm), the new sorting section had significantly lower retention probability for haddock up to 58 cm.

Fig. 7.

Discussion

Sorting grids and square mesh panels are common technical devices used to supplement codend size and species selection in demersal trawls (e.g. Catchpole and Revill, 2008; Krag et al., 2016, Lövgren et al., 2016; Jørgensen et al., 2006). Therefore, developing models that enable quantifying size selectivity and escape behaviour through these devices is important. In European demersal trawl fisheries, haddock is one of the most studied species and it is often used for the evaluation of dual size selection systems that include square mesh panels (Graham et al., 2001, 2003; Zuur et al. 2001; O'Neill et al., 2006; Fryer et al., 2016) or sorting grids (Kvamme and Isaksen, 2004; Grimaldo et al., 2015; Sistiaga et al., 2009, 2010, 2016). However, only some of these earlier studies modelled and quantified explicitly fish contact probability with the selectivity devices (Zuur et al. 2001; O'Neill et al., 2006; Sistiaga, 2010, 2016; Fryer et al., 2016). Considering contact probability with selection devices is important because it can help identify where potential challenges with the tested device lie. For a sorting grid or a square mesh panel that is not sorting as intended for example, estimating the contact can help identify if the reason for failure is linked to an erroneous choice in the bar spacing or mesh size, or if on the contrary, it is linked to the design or unsuccessful placement of the device in the gear. Moreover, considering length-dependency for the contact parameter contributes to further identify the selective properties of the device tested and behaviour of the species studied. In all previous studies, contact probability has been modelled by a contact parameter that did not account for potential length-dependency for the fish seeking escape through the selective devices.

Considering that several authors have successfully described the selective properties of sorting grids and square mesh panels on haddock using a length-independent contact parameter, we first modelled the selectivity of the sorting section tested in the present study using length-independent parameters. However, already the first analyses carried out demonstrated that such a simplified model could not describe the size selectivity of the section tested in the present study properly. Therefore, we used a more complex model that accounted for the potential effect of fish size to describe the probability of haddock contacting the sorting grid or the square mesh panel in the section. This model satisfactorily described the size selection in the grid and in the square mesh panel as well as the combined size selection for the new sorting section.

The results of the present study show that the probability for small haddock to seek escape through either the grid or the square mesh panel is higher than for bigger individuals that could have still escaped through the devices if they had made contact with them. Regarding the grid, our results are based on a grid placed with the outlet in the lower panel. Some studies have reported that smaller fish tend to remain closer to the lower panel than bigger fish of the same species when inside a trawl (Krag et al., 2014; Melli et al., 2018). This may be part of the reason for the size-dependent contact pattern observed in our study. However, bigger haddock may also be better at avoiding contact with obstacles or devices they may interpret as a threat than smaller fish due to superior swimming ability. Considering the result obtained in this study and the results reported by Krag et al. (2014), it would be valuable to repeat the present experiment with the grid positioned as it is in the Sort-V grid section, with the escape route upwards, to see if the contact pattern is reversed. Regarding the square mesh panel, it was estimated to have higher selectivity contact than the grid for all sizes of haddock above 25 cm. A potential explanation for the higher estimated panel selectivity contact could be related to the location of the square mesh panel and the fact that haddock has in numerous occasions been reported to seek escape upwards (Engås and Godø, 1989; Wardle, 1993; Beutel et al., 2008; Winger et al., 2010).

The findings that the smallest haddock are more likely to utilize an escape opportunity more efficiently than bigger fish that would still manage to escape through the sorting device if they attempted to do so, is in line with the findings of Grimaldo et at. (2018). These authors studied the size selectivity of haddock in a non-tapered four-panel square mesh section. In their experiments, Grimaldo et al. (2018) stablished which sizes of haddock would be able to escape through the panel conditioned that they made selectivity contact with it. The investigation was carried out for haddock >20 cm in length, and for each of the three configurations tested (i: no simulation device; ii: with mechanical simulation device; iii: mechanical and light simulation device) they found out that the escape attempt probability for haddock decreased with increasing fish length.

The haddock sampled in this experiment covered a wide range of sizes that, assuming they made selectivity contact with the selectivity devices in the section tested, would have at least some chance of escaping through them (10–58 cm). Compared to some of the former studies that did not sample haddock < 20 or 30 cm (Sistiaga et al., 2010, 2016) or used square mesh panels with smaller mesh sizes (Zuur et al. 2001; O'Neill et al., 2006; Fryer et al., 2016), the size range of haddock that could potentially escape through the sorting devices was much bigger in our study. This likely explains our need for a model that accounts for a length-dependent contact probability to estimate the selectivity of the selection devices in the sorting section. This premise is supported by our explorative analysis in which we ignored haddock below a specific but variable smaller size. The results of the analysis demonstrate that it is not necessary to account for length-dependency of the contact probability if haddock < 20 cm are ignored (Table 4; Fig. 6). However, this finding also illustrates the importance of not extrapolating results outside of the length range sampled. To our knowledge this is the first study that explicitly considers fish size-dependent contact probability in relation to grid and square mesh panel size selectivity. For this we adopted the flexible model for length-dependent contact proposed by Krag et al. (2014), who applied it for modelling escape through a panel with so big mesh size (800 mm) that all fish attempting escape would do so. In our case the situation is more complicated as the selectivity potential of the grid and square mesh panel will limit the sizes of haddock that would be able to escape. To our knowledge the current study is the first one using a length-dependent model for contact probability in relation to a size selection device. As demonstrated by the examples shown in Fig. 3, this combination of length-dependent contact probability and size selectivity of the device itself can lead to a variety of different size selection curves. This includes a so-called "cup-shaped" size selection curve with the lowest retention probability for medium sized fish and higher retention for both smaller and bigger fish. Further, the flexibility of our modelling approach and variety of size selection curves it can represent highlights the potential of the approach used, and may therefore be of relevance to model size selection for other species and/or selection devices in trawls and seines.

The size selectivity performance of the new sorting system was compared with previous obtained results for the two existing grid systems used today in the investigated fishery (Fig. 7). However, some caution needs to be taken when comparing with results obtained from former fishing cruises as potential differences in average fishing conditions may to some extent affect the size selective performance of the devices tested. Therefore, such comparison is only fully valid under the assumption that average fishing conditions were similar during the cruises in question or under the assumption that differences in fishing condition would not affect the selectivity performances of the devices being tested.

Acknowledgements

We are grateful to the crew of RV 'Helmer Hanssen' for their valuable help during the cruise. We also want to thank the Directorate of Fisheries, the Research Council of Norway (RCN project 243627), and the University of Tromsø for their financial support. Finally, we want to express our gratitude to the Editor and anonymous reviewers for their valuable comments during the review process which helped improving this manuscript greatly.

References

Akaike, H., 1974. A new look at the statistical model identification. IEEE Trans. Autom. Control 19: 716–723.

Alzorriz N., Arregi L., Herrmann B., Sistiaga M., Casey J., Poos J.J., 2016, Questioning the effectiveness of technical measures implemented by the Basque bottom otter trawl fleet: implications under the EU landing obligation. Fish. Res. 175: 116–126.

Beutel, D., Skrobe, L., Castro, K., Ruhle Sr., P., Ruhle Jr., P., O'Grady, J., Knight, J., 2008. Bycatch reduction in the Northeast USA directed haddock bottom trawl fishery. Fish. Res. 94: 190–198.

Brčić, J., Herrmann, B., Sala, A., 2016. Can a square-mesh panel inserted in front of the codend improve the exploitation pattern in Mediterranean bottom trawl fisheries? Fish. Res. 183:13-18.

Broadhurst, M.K. 2000. Modifications to reduce bycatch in prawn trawls: A review and framework for development. Rev. Fish. Biol. Fish. 10: 27–60. doi:10.1023/A:1008936820089.

Catchpole, T. L., Revill, A. S. 2008. Gear technology in Nephrops trawl fisheries. Reviews in Fish Biology and Fisheries, 18: 17–31.

Chernick, M.R., 2007. Bootstrap Methods: A guide for practitioners and researchers, second edition. Wiley series in probability and statistics. Wiley, New York.

Efron, B., 1982. The jackknife, the bootstrap and other resampling plans. SIAM Monograph No 38, CBSM-NSF.

Engås, A., Godø, O.R., 1989. The effect of different sweep lengths on the lengthcomposition of bottom-sampling trawl catches ICES J. Mar. Sci. 45: 263–268.

Fryer, R. J., 1991. A model of between-haul variation in selectivity. ICES J. Mar. Sci. 48: 281–290.

Fryer, R. J., O'Neill, F. G., Edridge, A., 2016. A meta-analysis of haddock size-selection data. Fish and Fisheries, 17: 358–374.

Gjøsund, S. H., 2012. Simplified approximate expressions for the boundary layer flow in cylindrical sections in plankton nets and trawls. Open Journal of Marine Science 2: 4.

Glass, C.W., 2000. Conservation of fish stocks through bycatch reduction: a review. Northeast Nat. 7: 395–410.

Graham, N., Kynoch, R. J., 2001. Square mesh panels in demersal trawls: some data on haddock selectivity in relation to mesh size and position. Fish. Res. 49: 207–218.

Graham, N., Kynoch, R. J., Fryer, R. J., 2003. Square mesh panels in demersal trawls: further data on haddock and whiting selectivity in relation to panel position. Fish. Res. 62: 361–375.

Grimaldo, E., Sistiaga, M., Herrmann, B., Gjøsund, S.H., Jørgensen, T., 2015. Effect of the lifting panel on selectivity of a compulsory grid section (Sort-V) used by the demersal trawler fleet in the Barents Sea cod fishery. Fish. Res. 170: 158–165.

Grimaldo, E., Sistiaga, M., Herrmann, B., Larsen, R.B., 2016. Trawl Selectivity in the Barents Sea Demersal Fishery. *In:* Fisheries and Aquaculture in the Modern World (edited by Mikkola, H.), INTECHhttp://dx.doi.org/10.5772/61558.

Grimaldo, E., Sistiaga, M., Herrmann, B., Larsen, R. B., Brinkhof, J., Tatone, I., 2018. Improving release efficiency of cod (*Gadus morhua*) and haddock (*Melanogrammus aeglefinus*) in the Barents Sea demersal trawl fishery by stimulating escape behaviour. Can. Journal Fish. Aquat. Sci. 75: 402-416.

Herrmann, B., Sistiaga, M., Larsen, R.B., Nielsen, K.N., 2013. Size selectivity of redfish (*Sebastes* spp.) in the Northeast Atlantic using grid-based selection systems for trawls. Aquat. Living Resour. 26: 109–120.

Isaksen, B., Gamst, K., Kvalsvik, K., Axelsen, B., 1998. Sammenligning av seleksjons- og brukeregenskapene hos Sort-X og enkelrist for topanels torsketrål. Forsøk utført ombord på M/Tr. "Anny Kræmer" ved Bjørnøya 15–28 August 1997. Institute of Marine Research, Bergen. (In norwegian).

Kelleher, K., 2005. Discards in the world's marine fisheries. An update. FAO Technical Paper No. 470, 131 pp.

Krag, L. A., Holst, R., Madsen, N., Hansen, K., Frandsen, R. 2010. Selective haddock (*Melanogrammus aeglefinus*) trawling: avoiding cod (*Gadus morhua*) bycatch. Fish. Res. 101: 20–26.

Krag, L.A., Herrmann, B., Feekings, J., Karlsen, J.D., 2016. Escape panels in trawls – a consistent management tool? Aquat. Living Resour. 29: 306. DOI: 10.1051/alr/2016028.

Krag, L.A., Herrmann, B., Feekings, J., Lund, H., Karlsen, J.D., 2017. Improving escape panel selectivity in Nephrops directed fisheries by actively stimulating fish behaviour. Can. Journal Fish. Aquat. Sci. 74: 486-493.

Krag, L.A., Herrmann, B., Karlsen, J., 2014. Inferring fish escape behaviour in trawls based on catch comparison data: Model development and evaluation based on data from Skagerrak, Denmark. PLoS ONE 9(2): e88819. doi:10.1371/journal.pone.0088819.

Kvamme, C., Isaksen, B., 2004. Total selectivity of a commercial cod trawl with and without a grid mounted: grid and codend selectivity of north-east Arctic cod. Fish. Res. 68: 305–318.

Larsen, R.B., Herrmann, B., Sistiaga, M., Grimaldo, E., Tatone, I., Onandia, I., 2016. Size selection of redfish (*Sebastes spp.*) in a double grid system: Quantifying escapement through individual grids and comparison to former grid trials. Fish. Res. 183: 385-395.

Larsen, R.B., Herrmann, B., Sistiaga, M., Grimaldo, E, J., Tatone, I., Brinkhof, 2018. Size selection of cod (*Gadus morhua*) and haddock (*Melanogrammus aeglefinus*) in the Northeast Atlantic bottom trawl fishery with a newly developed double steel grid system. Fish. Res. 201: 120-130.

Larsen, R.B., Isaksen, B., 1993. Size selectivity of rigid sorting grids in bottom trawls for Atlantic cod (*Gadus morhua*) and haddock (*Melanogrammus aeglefinus*). ICES Mar. Sci. Symp. 196: 178–182.

Lövgren, J., Herrmann, B., Feekings, J., 2016. Bell-shaped size selection in a bottom trawl: A case study for Nephrops directed fishery with reduced catches of cod. Fish. Res. 184: 26-35.

Melli, V., Karlsen, J., Feekings, J., Herrmann, B., Krag, L.A., 2017. FLEXSELECT: counter-herding device to reduce bycatch in crustacean trawl fisheries. Can. Journal Fish. Aquat. Sci, doi.org/10.1139/cjfas-2017-0226.

Melli, V., Krag, L.A., Herrmann, B., Karlsen, J.D., 2018. Investigating fish behavioural responses to LED lights in trawls and potential applications for bycatch reduction in the Nephrops-directed fishery. ICES J. Mar. Sci.: doi.org/10.1093/icesjms/fsy048.

O'Neill, F.G., Kynoch, R.J., Fryer, R.J., 2006. Square mesh panels in North Sea demersal trawls: separate estimates of panel and cod-end selectivity. Fish. Res.78, 333–341.

Santos, J., Herrmann, B., Otero, P., Fernandez, J., Pérez, N., 2016. Square mesh panels in demersal trawls: Does the lateral positioning enhance fish contact probability? Aquat. Living Resour. 29: 302. DOI: 10.1051/alr/2016025.

Sistiaga, M., Brinkhof, J., Herrmann, B., Grimaldo, E., Langård, L., Lilleng, D., 2016. Size selective performance of two flexible sorting grid designs in the Northeast Arctic cod (*Gadus morhua*) and haddock (*Melanogrammus aeglefinus*) fishery. Fish. Res. 183: 340-351.

Sistiaga, M., Herrmann, B., Grimaldo, E., Larsen, R.B., 2010. Assessment of dual selection in grid based selectivity systems. Fish. Res. 105: 187-199.

Sistiaga, M., Herrmann, B., Larsen, R.B., 2009. Investigation of the paired-gear method in selectivity studies. Fish. Res. 97: 196–205.

Sistiaga, M., Herrmann, B., Grimaldo, E., Larsen, R.B., Olsen, L., Brinkhof, J., Tatone, I., 2017. Combination of a sorting grid and a square mesh panel to optimize size selection in the North-East Arctic cod (*Gadus morhua*) and redfish (*Sebastes spp*) trawl fisheries. ICES J. Mar. Sci. 75: 1105-1116.

Wardle, C.S. 1993. Fish behaviour and fishing gear. In Behaviour of teleost fishes. 2nd ed. Edited by T. Pitcher. Chapman and Hall, London. pp. 609–643. ISBN 978-0-412-42930-9.

Westhoff, C.J.W., Pope, J.A., Beverton, R.J.H. 1962. The ICES mesh gauge. Charlottenlund Slot, Charlottenlund, Denmark. 15 pp.

Wileman, D. A., Ferro, R. S. T., Fonteyne, R., Millar, R. B. (Eds.), 1996. Manual of methods of measuring the selectivity of towed fishing gears. ICES Cooperative Research Report No. 215.

Winger, P.D., Eayrs, S., Glass, C.W., 2010. Fish behaviour near bottom trawls. In: He,P. (Ed.), Behaviour of Marine Fishes: Capture Processes and Conservation Challenges. Wiley–Blackwell, Ames, IA, pp. 67–103.

Zuur, G., Fryer, R.J., Ferro, R.S.T., Tokai, T., 2001. Modelling the size selectivities of a trawl codend and an associated square mesh panel. ICES J. Mar. Sci. 58: 657–671.

FIGURE CAPTIONS

Fig. 1: Schematic representation of the experimental grid section with the square mesh panel at the top.

Fig. 2: Technical specification of the covers used over the outlet of the grid and the square mesh panel. The picture below shows a snapshot of the tests carried out with the section and the covers in the flume tank prior to the tests at sea. Note that the kites used in the cover over the square mesh panel in the tests in the flume tank were replaced by six 20 cm floats during the trials at sea. The floats were fixed as specified in the drawing.

Fig. 3: Examples on different device contact curves simulated based on model (2) (left column) and the associated size selection curves (retention curves) (right column) based on model (1). A: low and constant contact ($C1_{device} = C2_{device} = 0.2$). B: high and constant contact ($C1_{device} = C2_{device} = 0.8$). C: slow increasing contact ($C1_{device} = 0.2$; $C2_{device} = 0.8$; $L50C_{device} = 30$ cm; $SRC_{device} = 30$ cm). D: fast increasing contact ($C1_{device} = 0.2$; $C2_{device} = 0.8$; $L50C_{device} = 20$ cm; $SRC_{device} = 10$ cm). E: slow decreasing contact ($C1_{device} = 0.9$; $C2_{device} = 0.3$; $L50C_{device} = 30$ cm; $SRC_{device} = 40$ cm). F: fast increasing contact ($C1_{device} = 0.9$; $C2_{device} = 0.3$; $L50C_{device} = 25$ cm; $SRC_{device} = 8$ cm). For all selection curves $L50_{device} = 45$ cm and $SR_{device} = 8$ cm were used together with the contact model shown in the left column for the specific row.

Fig. 4: Panels a, b, and c show escape probabilities through the grid, escapement through the square mesh panel, and combined retention in the codend, respectively, using model (1) and assuming length-independent contact probabilities with the grid and square mesh panel. Panels d, e, and f show the same except the contact probabilities with the grid and the square mesh panel were modelled as length-dependent according to equation (2). Circle marks

represent the experimental rates, and the thick curve represents the modelled rate based on equation (1). The stippled curves show 95% confidence limits for the modelled rate. The dotted curve represents the population found in each specific compartment (grid cover, square mesh panel cover, and codend).

Fig. 5: Grid, square mesh panel stand-alone size selection, and estimated selectivity contact. a: grid size selection curve (black curve). b: square mesh panel size selection (black curve). c: Selectivity contact curve for the grid. d: Selectivity contact curve for the square mesh panel. The stippled curves show 95% confidence limits for the selectivity curve or selectivity contact curve. Circle marks represent the experimental rates. Dotted grey and black curve represent the population of haddock entering and being retained in that step of the size selection process, respectively.

Fig. 6: First, second, and third columns show grid size selectivity, square mesh panel selectivity, and combined retention in codend, respectively, using model (1) and assuming haddock length-independent contact probabilities with the grid and square mesh panel. Circle marks represent the experimental rates and the thick curve represents the modelled rate based on equation (1). From top to bottom rows, haddock < 10, 15, 20, 25, and 30 cm, respectively, were excluded from the analysis.

Fig. 7: Comparison of size selectivity for the new sorting section (black curve) versus existing sorting sections (grey curves). The stippled curves show 95% confidence limits for the selectivity curve. a: Comparison with results for Flexigrid (grey curve) presented in Sistiaga et al. (2016). b: Comparison with results for the Sort-V grid presented in Sistiaga et al. (2010).

FIG. 1

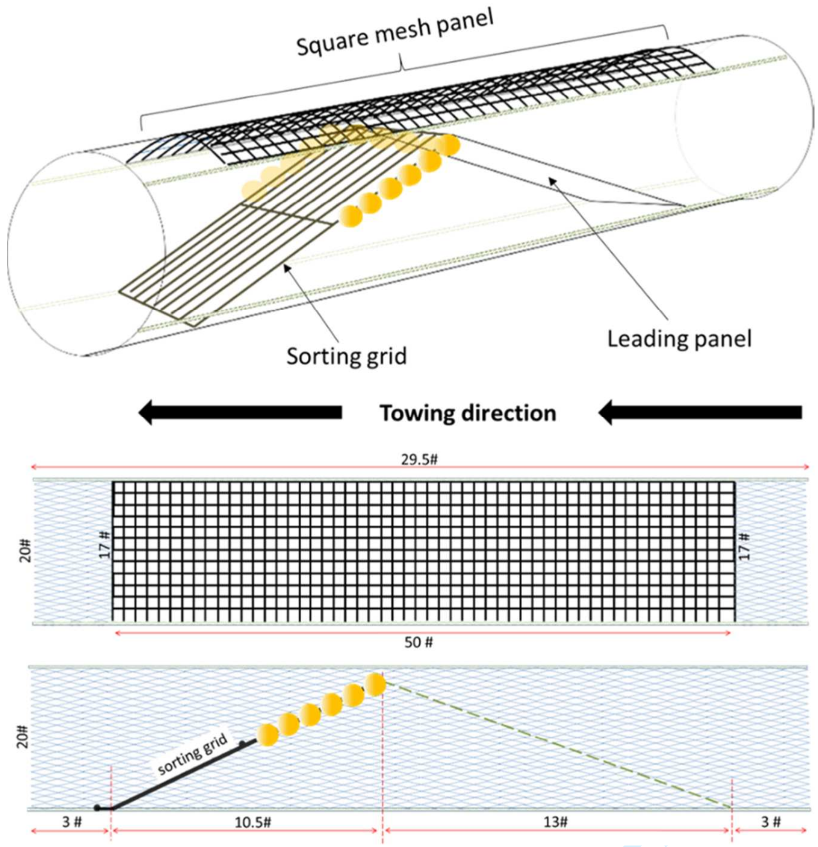
Square mesh panel
Sorting grid
Leading panel
Towing direction
29.5#
20#
17#
17#
50 #
20#
sorting grid
3 #
10.5#
13#
3 #

FIG. 2

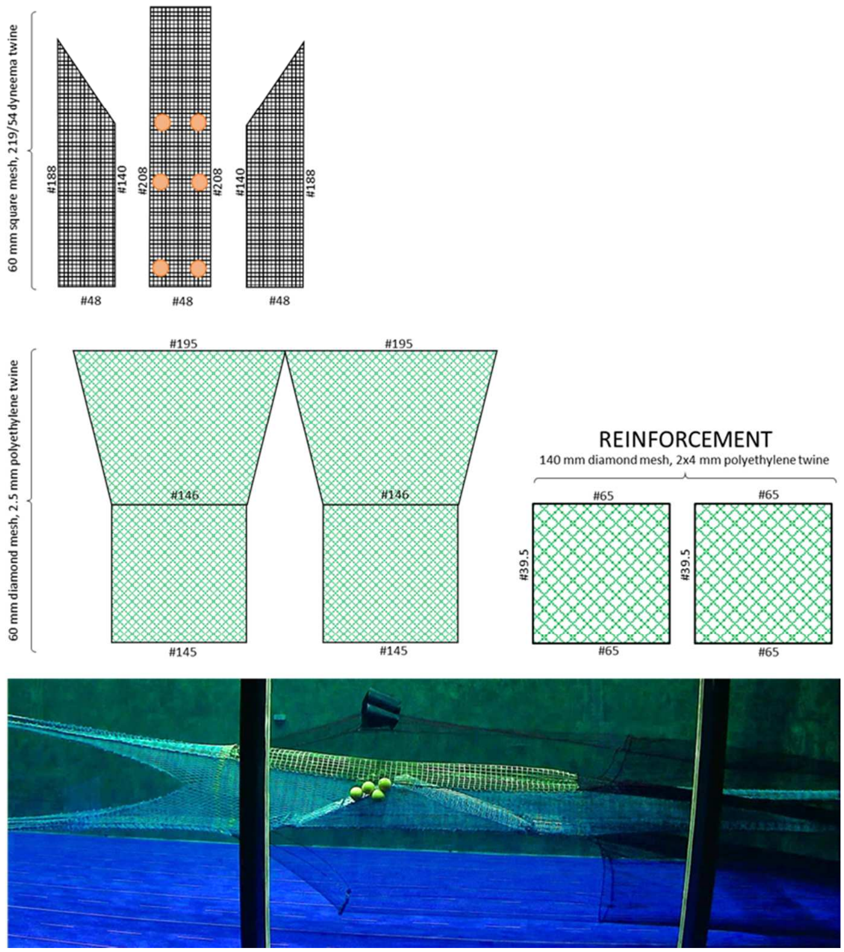
60 mm square mesh, 219/54 dyneema twine
#188
#140
#208
#208
#140
#188
#48
#48
#48
60 mm diamond mesh, 2.5 mm polyethylene twine
#195
#195
#146
#146
#145
#145
REINFORCEMENT
140 mm diamond mesh, 2x4 mm polyethylene twine
#65
#65
#39.5
#39.5
#65
#65

57 Fig. 3

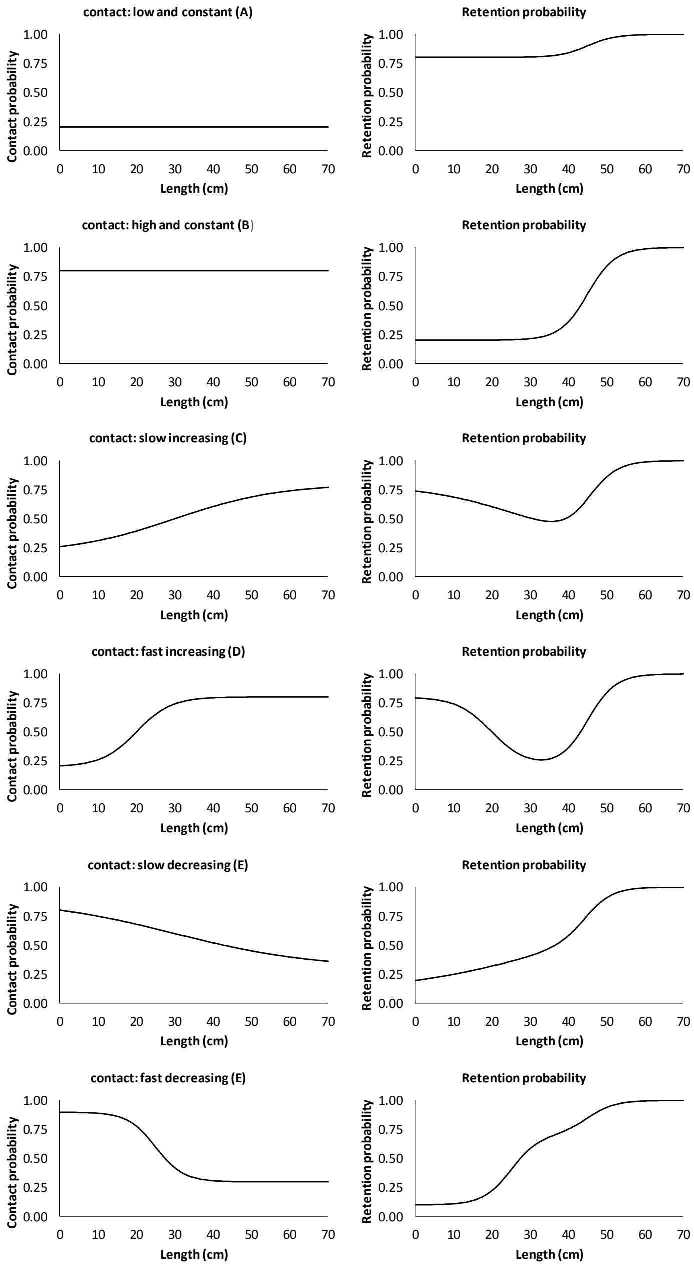
contact: low and constant (A)
Retention probability
contact: high and constant (B)
Retention probability
contact: slow increasing (C)
Retention probability
contact: fast increasing (D)
Retention probability
contact: slow decreasing (E)
Retention probability
contact: fast decreasing (E)
Retention probability
Contact probability
Retention probability
Length (cm)
0.00
0.25
0.50
0.75
1.00
0
10
20
30
40
50
60
70

58

FIG. 4

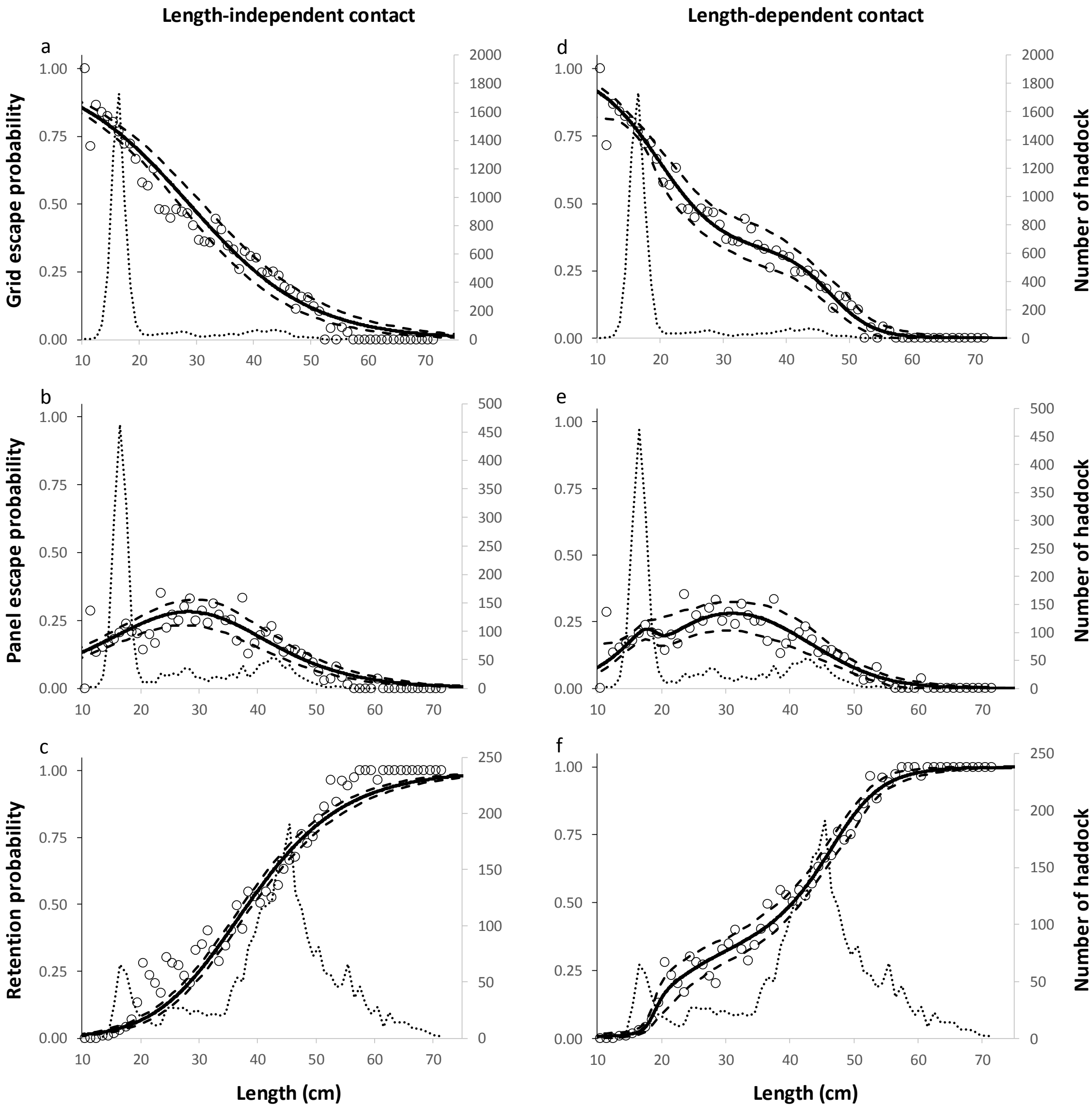

Length-independent contact
Length-dependent contact
a
b
c
d
e
f
Grid escape probability
Panel escape probability
Retention probability
Number of haddock
Length (cm)

63 FIG. 5

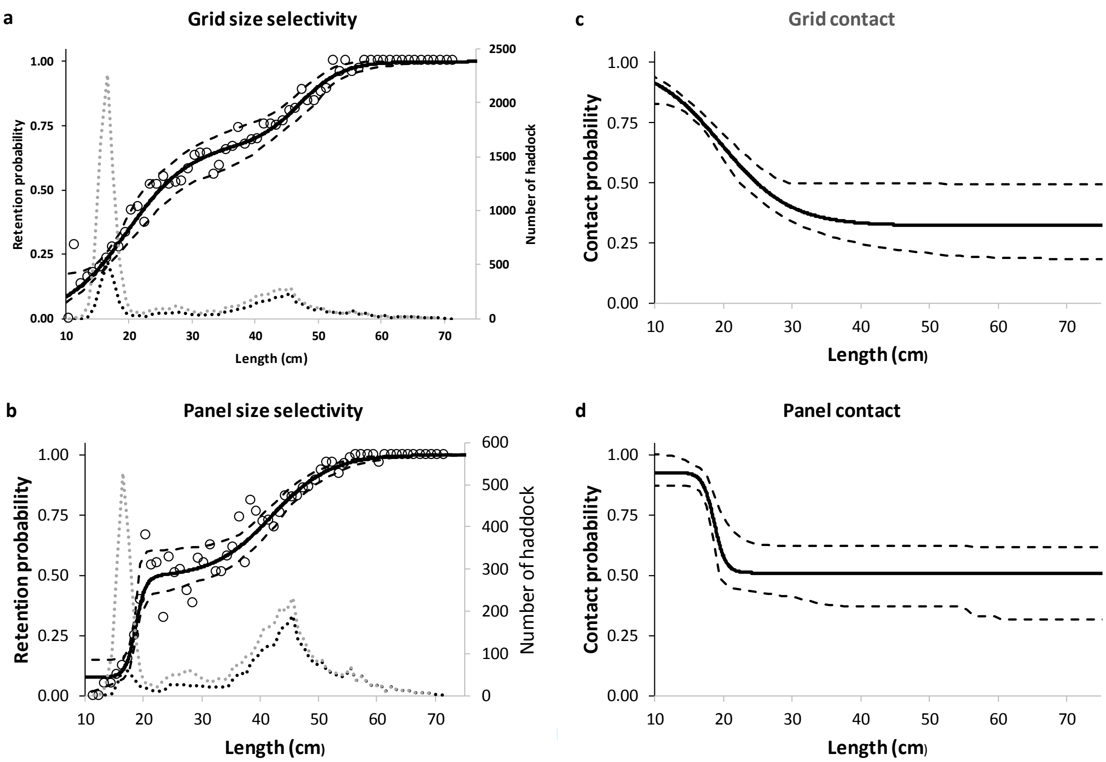
a
Grid size selectivity
Retention probability
Number of haddock
Length (cm)
b
Panel size selectivity
Retention probability
Number of haddock
Length (cm)
c
Grid contact
Contact probability
Length (cm)
d
Panel contact
Contact probability
Length (cm)

64

65

FIG. 6

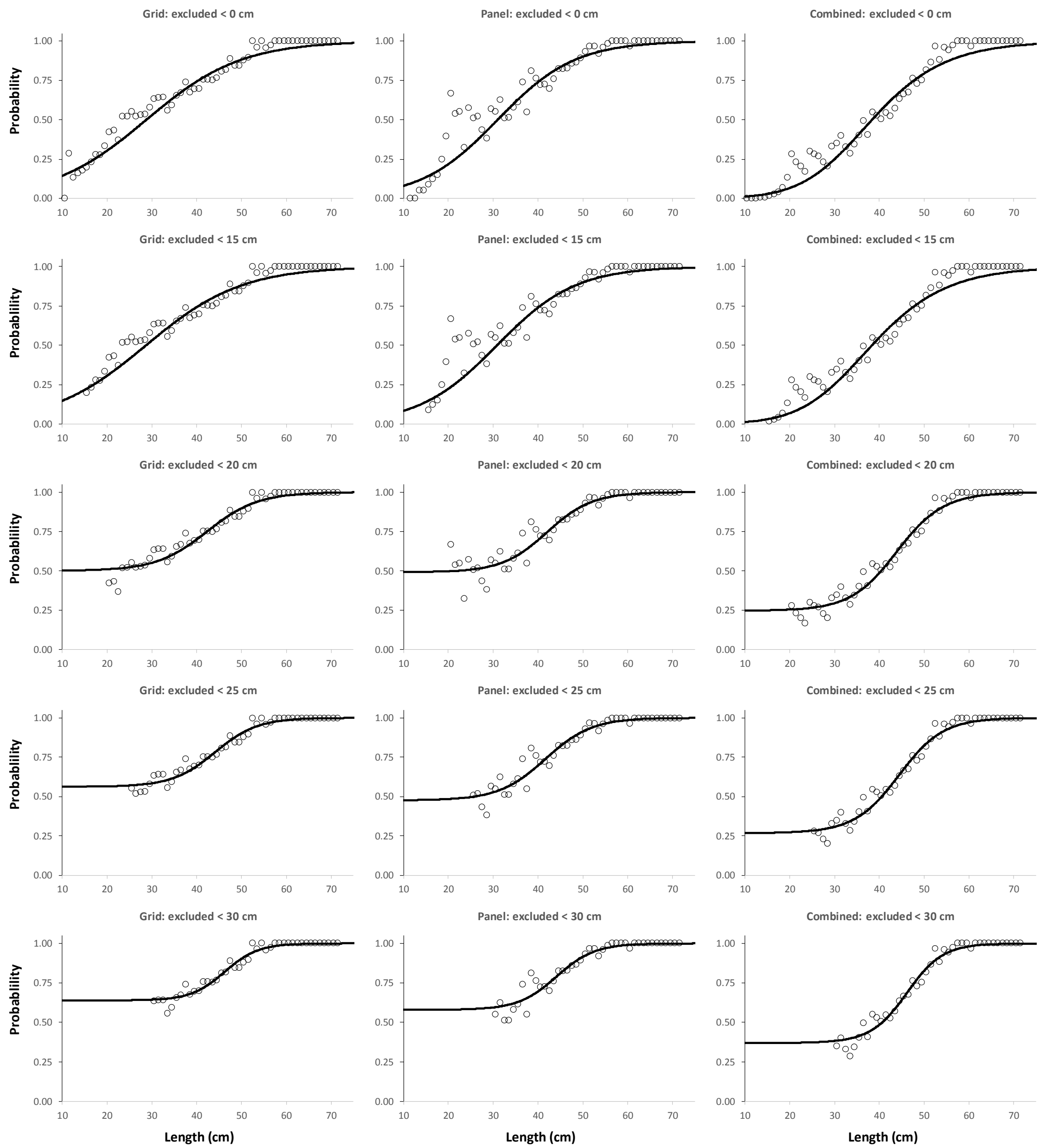
Grid: excluded < 0 cm
Panel: excluded < 0 cm
Combined: excluded < 0 cm
Grid: excluded < 15 cm
Panel: excluded < 15 cm
Combined: excluded < 15 cm
Grid: excluded < 20 cm
Panel: excluded < 20 cm
Combined: excluded < 20 cm
Grid: excluded < 25 cm
Panel: excluded < 25 cm
Combined: excluded < 25 cm
Grid: excluded < 30 cm
Panel: excluded < 30 cm
Combined: excluded < 30 cm
Probability
0.00
0.25
0.50
0.75
1.00
10
20
30
40
50
60
70
Length (cm)

FIG. 7

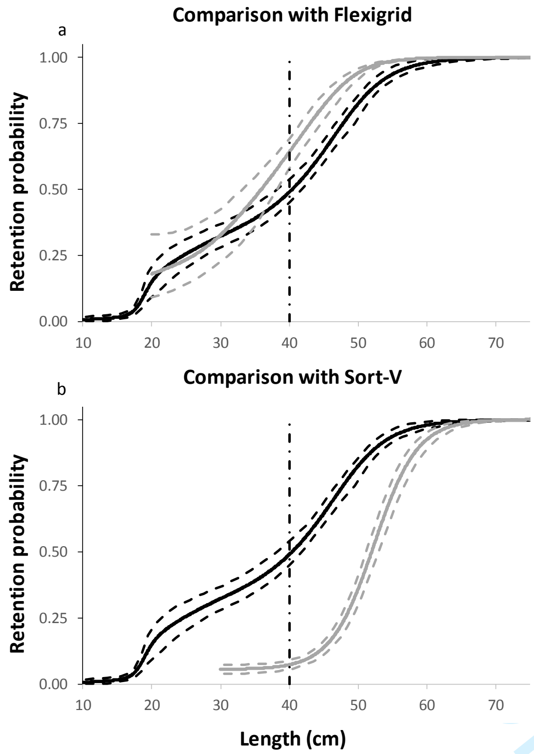
Comparison with Flexigrid
a
Retention probability
1.00
0.75
0.50
0.25
0.00
10
20
30
40
50
60
70
Comparison with Sort-V
b
Retention probability
1.00
0.75
0.50
0.25
0.00
10
20
30
40
50
60
70
Length (cm)

Table 1: Number of haddock caught and length measured in individual hauls conducted during this study. *ng*: number in cover over the grid; *np*: number in cover over the square mesh panel; *nc*: number in the blinded codend.

Haul	*ng*	*np*	*nc*
1	65	63	84
2	37	43	44
3	8	1	3
4	163	37	212
5	574	166	210
6	459	176	124
7	481	150	144
8	1064	406	301
9	245	96	243
10	218	50	59
11	178	52	55
12	662	99	258
13	561	217	139
14	255	85	188
15	189	89	131
16	190	61	135
17	271	77	156
18	478	193	136
19	114	26	63
20	105	40	60
sum	6317	2127	2745

Table 2: Statistics for the fit of model (1) considering constant contact probabilities (length-independent contact) and size-dependent contact probability, respectively, as described by model (2) (length-dependent contact). Statistics were calculated for the combined size selection in the sorting section (combined), for the grid size selection alone (grid), and for the square mesh panel alone (square mesh panel). DOF denotes degree of freedom.

Model		Grid	Square mesh panel	Combined
Length-independent contact	AIC-value	11971.23	4487.70	16458.93
	p-value	< 0.0001	< 0.0001	< 0.0001
	Deviance	118.60	163.27	281.86
	DOF	59	58	118
Length-dependent contact	AIC-value	11897.67	4395.07	16292.74
	p-value	0.9587	0.1754	0.6763
	Deviance	39.04	64.64	103.68
	DOF	56	55	111

Table 3: Parameter values for the model with length-dependent device contact. Values in parentheses are 95% confidence limits.

Device	Grid	Square mesh panel
$C1_{device}$	1.00 (0.82–1.00)	0.93 (0.87–1.00)
$C2_{device}$	0.32 (0.19–0.49)	0.51 (0.28–0.62)
$L50C_{device}$ *(cm)*	19.71 (17.74–23.46)	18.68 (17.83–23.04)
SRC_{device} *(cm)*	11.00 (4.36–16.73)	1.83 (0.00–9.62)
$L50_{device}$ (cm)	47.14 (41.95–51.37)	41.98 (37.87–47.67)
SR_{device} (cm)	7.48 (3.28–12.26)	11.12 (5.93–14.77)

Table 4: Fit statistics for length-independent contact model when data for haddock below specific lengths were excluded.

Data excluded below length (cm)	Grid			Panel			Combined		
	p-value	Deviance	DOF	p-value	Deviance	DOF	p-value	Deviance	DOF
0	< 0.0001	118.60	59	< 0.0001	163.27	58	< 0.0001	281.86	118
15	< 0.0001	113.00	54	< 0.0001	153.99	54	< 0.0001	266.98	108
20	0.3731	51.58	49	0.1611	58.72	49	0.1863	110.30	98
25	0.6779	39.18	44	0.2786	49.03	44	0.4737	88.21	88
30	0.8268	30.68	39	0.4121	40.31	39	0.7002	70.99	78